AEM
Journals.ASM.org

U(VI) Reduction by Diverse Outer Surface *c*-Type Cytochromes of *Geobacter sulfurreducens*

Roberto Orellana,[a] Janet J. Leavitt,[b] Luis R. Comolli,[c] Roseann Csencsits,[c] Noemie Janot,[d] Kelly A. Flanagan,[a] Arianna S. Gray,[a] Ching Leang,[a] Mounir Izallalen,[a] Tünde Mester,[a] Derek R. Lovley[a]

Department of Microbiology, University of Massachusetts, Amherst, Massachusetts, USA[a]; Department of Civil Engineering, University of New Mexico, Albuquerque, New Mexico, USA[b]; Life Sciences Division, Lawrence Berkeley National Laboratory, Berkeley, California, USA[c]; SLAC National Accelerator Laboratory, Menlo Park, California, USA[d]

Early studies with *Geobacter sulfurreducens* suggested that outer-surface *c*-type cytochromes might play a role in U(VI) reduction, but it has recently been suggested that there is substantial U(VI) reduction at the surface of the electrically conductive pili known as microbial nanowires. This phenomenon was further investigated. A strain of *G. sulfurreducens*, known as Aro-5, which produces pili with substantially reduced conductivity reduced U(VI) nearly as well as the wild type, as did a strain in which the gene for PilA, the structural pilin protein, was deleted. In order to reduce rates of U(VI) reduction to levels less than 20% of the wild-type rates, it was necessary to delete the genes for the five most abundant outer surface *c*-type cytochromes of *G. sulfurreducens*. X-ray absorption near-edge structure spectroscopy demonstrated that whereas 83% ± 10% of the uranium associated with wild-type cells correspond to U(IV) after 4 h of incubation, with the quintuple mutant, 89% ± 10% of uranium was U(VI). Transmission electron microscopy and X-ray energy dispersion spectroscopy revealed that wild-type cells did not precipitate uranium along pili as previously reported, but U(IV) was precipitated at the outer cell surface. These findings are consistent with those of previous studies, which have suggested that *G. sulfurreducens* requires outer-surface *c*-type cytochromes but not pili for the reduction of soluble extracellular electron acceptors.

The mechanisms for U(VI) reduction in *Geobacter* species are of interest because the precipitation of U(VI) to U(IV) is a promising strategy for the *in situ* bioremediation of uranium-contaminated groundwater, and *Geobacter* species often predominate in subsurface environments in which U(VI) reduction is stimulated with the addition of organic electron donors (1, 2). The suggestion that electrons are directly transferred from the conductive pili of *Geobacter sulfurreducens* to U(VI) (3, 4) contrasts with the finding that pili are not required for the reduction of other soluble extracellular electron acceptors, such as Fe(III) citrate or the humic substances analog anthraquinone-2,6-disulfonate (AQDS) (5, 6).

Pili are required for long-range electron transport to insoluble electron acceptors in the *Geobacter* species that have been examined to date. This includes reduction of insoluble Fe(III) oxides (5, 7) and electron exchange between syntrophic partners (8, 9), as well as electron conduction through current-producing biofilms (10–12). This has been attributed to the metallic-like conductivity of the pili (12, 13). For example, a strain of *G. sulfurreducens*, designated Aro-5, which was genetically modified to produce pili with diminished conductivity lacked the capacity for effective Fe(III) oxide reduction and current production (13). In addition to pili, *G. sulfurreducens* requires the multiheme *c*-type cytochrome, OmcS, for Fe(III) oxide reduction (14). OmcS is specifically localized on the pili (15). Thus, the simplest model for the last steps in Fe(III) oxide reduction is electron transport to OmcS via the pili, with OmcS facilitating electron transfer from the pili to Fe(III) oxide (16, 17). In a similar manner, networks of pili facilitate long-range electron transport through conductive biofilms of *G. sulfurreducens*, but one or more multiheme cytochromes are required to promote electron transfer from the biofilm to electrodes (11, 18, 19).

Gene deletion studies demonstrated that in contrast to the requirement of OmcS for Fe(III) oxide reduction, OmcS was not essential for the reduction of Fe(III) citrate or AQDS (6, 14), consistent with the ability of the pilus-deficient strain to reduce these electron acceptors (5, 6). In order to significantly reduce the capacity for AQDS reduction, it was necessary to delete the genes for five outer-surface *c*-type cytochromes in one strain (6). These included OmcS and the OmcS homolog OmcT, as well as OmcE, OmcZ, and OmcB. Immunolabeling studies have demonstrated that OmcB is embedded in the outer membrane of *G. sulfurreducens*, with a portion of the molecule exposed to the extracellular environment (20), whereas OmcZ (19) and OmcE (14) are localized in the extracellular matrix. The necessity to remove all of these cytochromes suggested that AQDS reduction is rather nonspecific. Although deleting just OmcB significantly eliminated the capacity for Fe(III) citrate reduction (21), the OmcB-deficient mutant adapted over time to reduce Fe(III) citrate in the absence of OmcB, with increased expression of other outer-surface cytochromes (22).

A diversity of *c*-type cytochromes can reduce U(VI) *in vitro* (18, 23–25). Furthermore, *c*-type cytochromes are essential for U(VI) reduction in *Shewanella oneidensis*, which accumulates uranium nanoparticles in association with the outer membrane cytochromes (25). Previous studies also suggested that *c*-type cytochromes exposed on the outer surface of *G. sulfurreducens* were involved in U(VI) reduction (26). An important line of evidence for a potentially important role of pili in U(VI) reduction was the

Received 30 July 2013 Accepted 5 August 2013
Published ahead of print 9 August 2013
Address correspondence to Roberto Orellana, orellana@microbio.umass.edu.
Supplemental material for this article may be found at http://dx.doi.org/10.1128/AEM.02551-13.

doi:10.1128/AEM.02551-13

finding that a *pilA*-deficient mutant reduced U(VI) at a rate ca. one-third the rate at which the wild type reduced U(VI) (3). However, the *pilA*-deficient mutant was also defective in the production of outer-surface *c*-type cytochromes (3), confounding interpretation of the results. These considerations and the recent availability of the Aro-5 strain led us to further investigate the hypothesis that pili are a major conduit for electron transfer to U(VI) by *G. sulfurreducens*.

MATERIALS AND METHODS

Bacterial strains, culture conditions, and cell suspensions. All strains (see Table S1 in the supplemental material) were obtained from our laboratory collection and were routinely cultured anaerobically in medium with 10 mM acetate as an electron donor and 20 mM fumarate as an electron acceptor, as previously described (26).

Resting cell suspensions were prepared as previously described (26). Briefly, cells were harvested in late exponential phase with an optical density of 0.25 to 0.28, washed with buffer, and resuspended in buffer containing $NaHCO_3$ (2.5 g liter^{-1}), NH_4Cl (0.25 g liter^{1}), $NaH_2PO_4 \cdot H_2O$ (0.006 g liter^{-1}), and KCl (0.1 g liter^{-1}) at an optical density at 600 nm (OD_{600}) of 0.075 to 0.08. Acetate (5 mM) and uranyl acetate (1 mM) were added as an electron donor and acceptor, respectively. Heat-killed controls were prepared by autoclaving the cell suspension for 30 min before the addition of U(VI). Cell suspensions were incubated at 30°C.

The ability of cells to reduce U(VI) was monitored as the loss of U(VI) over time as previously described (26). Briefly, samples from cell suspensions (100 μl) were taken at 1-h intervals and diluted in 14.9 ml of anoxic 100 mM bicarbonate and 14.9 ml of anoxic Uraplex working solution. U(VI) concentrations were quantified using a kinetic phosphorescence analyzer (KPA) (Chemcheck Corp., Richland, WA), and the rate of enzymatic U(VI) reduction over 4 h was calculated as described previously (26).

TEM. For a control survey of cell appendages, cells were harvested by centrifugation at mid-log phase and prepared as previously described (26). Samples were placed on 400-mesh carbon-coated copper grids, incubated for 5 min, and then stained with 2% uranyl acetate. Cell appendages were observed with a Jeol 100 transmission electron microscope (TEM) at an accelerating voltage of 80 kV. Images were taken digitally using the MaxIm-DL software and analyzed using the software program ImageJ (http://rsbweb.nih.gov/ij/index.html).

For cryo-TEM, 5 μl-aliquots of culture were placed on lacey carbon grids (Ted Pella 01881; Ted Pella Inc., Redding, CA) that were pretreated by glow discharge. The Formvar support was not removed from the lacey carbon. The grids were manually blotted with filter paper, flash frozen with a portable cryoplunger (27), and stored in liquid nitrogen.

For air-dried samples, aliquots of 5 μl (each) were placed on continuous carbon-coated Formvar TEM) pretreated grids (Ted Pella 01753; Ted Pella Inc., Redding, CA) by glow discharge. They were blotted after equilibration for 2 min. Cryogrids were freeze-dried after cryo-TEM imaging. Both air-dried and freeze-dried cryo-TEM specimens were used for X-ray energy dispersion spectroscopy (XEDS) analysis as described below.

Cryo-TEM images were acquired on a Jeol 3100-FFC electron microscope equipped with a field emission gun (FEG) electron source operating at 300 kV, an Omega energy filter, a cryotransfer stage, and a Gatan 795 4,000 (4K) × 4K charge-coupled-device (CCD) camera mounted at the exit of an electron decelerator held at a constant voltage of 200 kV (28). The stage was cooled with liquid nitrogen to 80 K during acquisition of all data sets. In order to have a statistically relevant survey, more than 100 images were recorded using magnifications of ×112K, ×70K, or ×42 at the CCD, giving a pixel size of 0.14 nm, 0.21 nm, or 0.375 nm at the specimen, respectively. Under-focus values ranged between 2 μm ± 0.5 μm to 12 μm ± 0.5 μm, and energy filter widths were typically around 28 eV ± 2 eV. The survey of the grids and the selection of suitable targets for tilt series acquisition were done in low-dose diffraction mode through the acquisition of dozens of images.

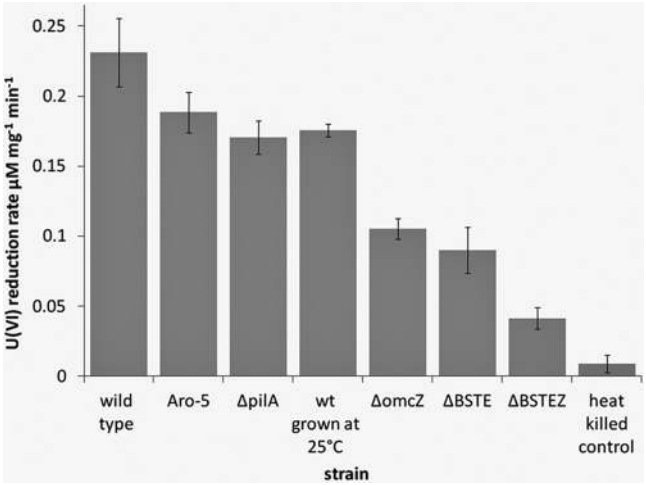

FIG 1 U(VI)-reducing activities of wild-type (wt) and mutant strains of *G. sulfurreducens*. Data are means ± standard deviations (SD) for triplicates.

Two tomographic data sets of Δ*pilA* were acquired. Tomographic tilt series were acquired under low-dose conditions, over an angular range between + 62° and −62°, ± 2° with increments of 2°. Sixty and sixty-three images were recorded for these tilt series, acquired semiautomatically with the software program Serial-EM (http://bio3d.colorado.edu/), adapted for Jeol microscopes. For these tilt series data sets, images were recorded using nominal magnification of ×15K, resulting in ×42K at the CCD and a pixel size of 0.375 nm at the specimen. The under-focus value was set to 12 μm ± 0.5 μm, and energy filter widths were set to 28 eV. The maximum dose used per complete tilt series was approximately 140 $e^-/Å^2$.

X-ray EDS. High-spatial-resolution chemical analyses of cell membranes of air-dried samples on continuous carbon-coated Formvar TEM grids and freeze-dried cryo-TEM samples were carried out in a Jeol 2100-F 200-kV field-emission analytical TEM equipped with an Oxford Inca energy-dispersive spectroscopy (EDS) X-ray detection system at the Molecular Foundry at Lawrence Berkeley National Laboratory. High-angle annual dark field (HAADF) scanning transmission electron microscopy (STEM) images and X-ray elemental line scans were acquired with a 1-nm probe at 120 or 200 kV. The specimens were tilted 10 degrees toward the X-ray detector to optimize the X-ray detection geometry. Collection times were 300 live seconds for each line scan. The EDS line scans on the high-contrast regions of the outer membrane clearly demonstrate the localized uranium in this membrane responsible for the increased contrast in the STEM HAADF images.

Software. All tomographic reconstructions were obtained with the program Imod (http://bio3d.colorado.edu/) (29). The program ImageJ (NIH; http://rsb.info.nih.gov/ij/) was used for analysis of the two-dimensional (2D) image projections. Volume rendering and image analysis of tomographic reconstructions was performed using the open source program ParaView (http://www.paraview.org/), and movies were created using the open source package ffmpeg (http://www.ffmpeg.org/). The inner membranes of 2 cells of each species were segmented by hand using the program Imod.

XANES analyses. The oxidation state of uranium in cell suspension samples was determined with the X-ray absorption near-edge structure (XANES) spectroscopic method. Cell pellets from the cell suspensions were flash frozen in liquid nitrogen and shipped on ice. Samples were loaded in aluminum sample holder with Kapton windows in an anaerobic chamber (2 to 5% hydrogen, balance nitrogen) at the Stanford Synchrotron Radiation Lightsource (SSRL) (SLAC National Accelerator Laboratory, Menlo Park, CA). Immediately prior to analysis, the sample assembly was mounted in a liquid nitrogen cryostat, placed under vacuum, and

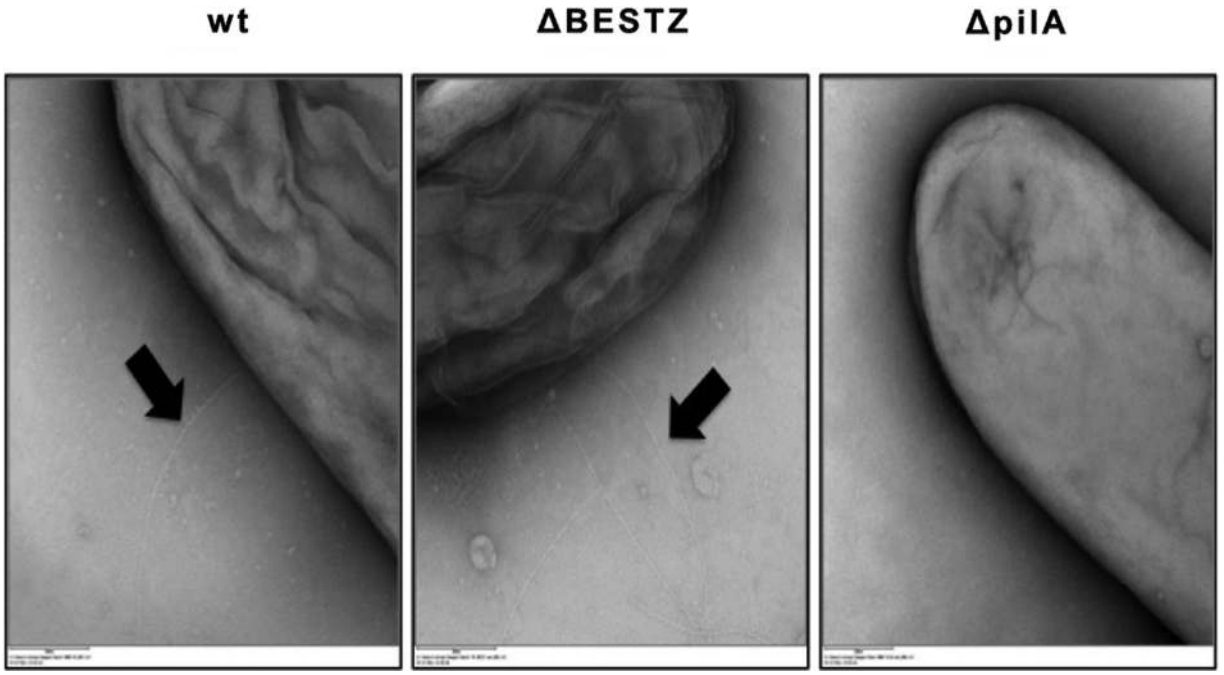

FIG 2 TEM pictures showing the levels of filament production in the wild type (left), the ΔBESTZ mutant (middle), and the Δ*pilA* mutant (right).

frozen. U L_{III}-edge transmission spectra were collected at SSRL beamline 4-1, using a Si(220) double-crystal monochromator detuned to reject higher harmonic intensity. Vertical slits in the experimental hutch were set to 0.5 mm during the measurement to ensure that the spectrometer resolution was lower than that of the intrinsic core-hole lifetime limitation. Energy calibration was monitored continuously, and no drift was detected. XANES spectra were background subtracted and analyzed using the ATHENA software program (30).

qRT-PCR. Total RNA was extracted using an RNeasy minikit (Qiagen) from mid-log acetate-fumarate cultures. cDNA was generated using the Enhanced Avian First Strand synthesis kit (Sigma-Aldrich, St. Louis, MO, USA) using random primers according to the manufacturer's recommendations. The SYBR green PCR master mix (Applied Biosystems, Foster City, CA) and the ABI 7500 real-time PCR system were used to amplify and to quantify PCR products from *pilA* with the primer pair RT_ORF02545_F and RT_ORF02545_R (11). Expression of this gene was normalized with expression of *proC*, a constitutively expressed gene in *G. sulfurreducens*, using the proC2F and proC77R primer pair. Relative levels of expression of the studied genes were calculated by the $2-\Delta\Delta C_T$ method (31).

RESULTS AND DISCUSSION

U(VI) reduction with genetically modified strains. Strain Aro-5, which produces pili with diminished conductivity but still properly localizes outer surface *c*-type cytochromes (13), reduced U(VI) at rates that were only slightly lower than and not significantly different from the wild-type rate of 0.23 μM U(VI) mg^{-1} min^{-1} (Fig. 1). This result suggested that electron conduction along pili was not an important requirement for U(VI) reduction.

With further investigation, we could not replicate the previously reported findings (3) that the *pilA*-deficient mutant had substantially lower rates of U(VI) reduction than the wild type or that pregrowing cells at 25°C, a temperature suggested to increase pilus production (3), significantly enhanced U(VI) reduction (Fig. 1).

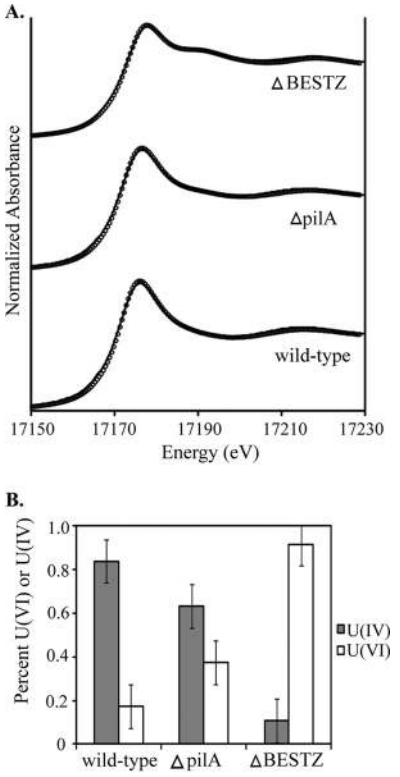

FIG 3 (A) Uranium LIII-edge XANES spectra of uranium associated with 3 strains of *G. sulfurreducens* (circles) and their corresponding fits (lines). (B) Proportions of uranium at the different oxidation states: U(IV) (gray bars) and U(VI) (white bars) after 4-h cell suspensions.

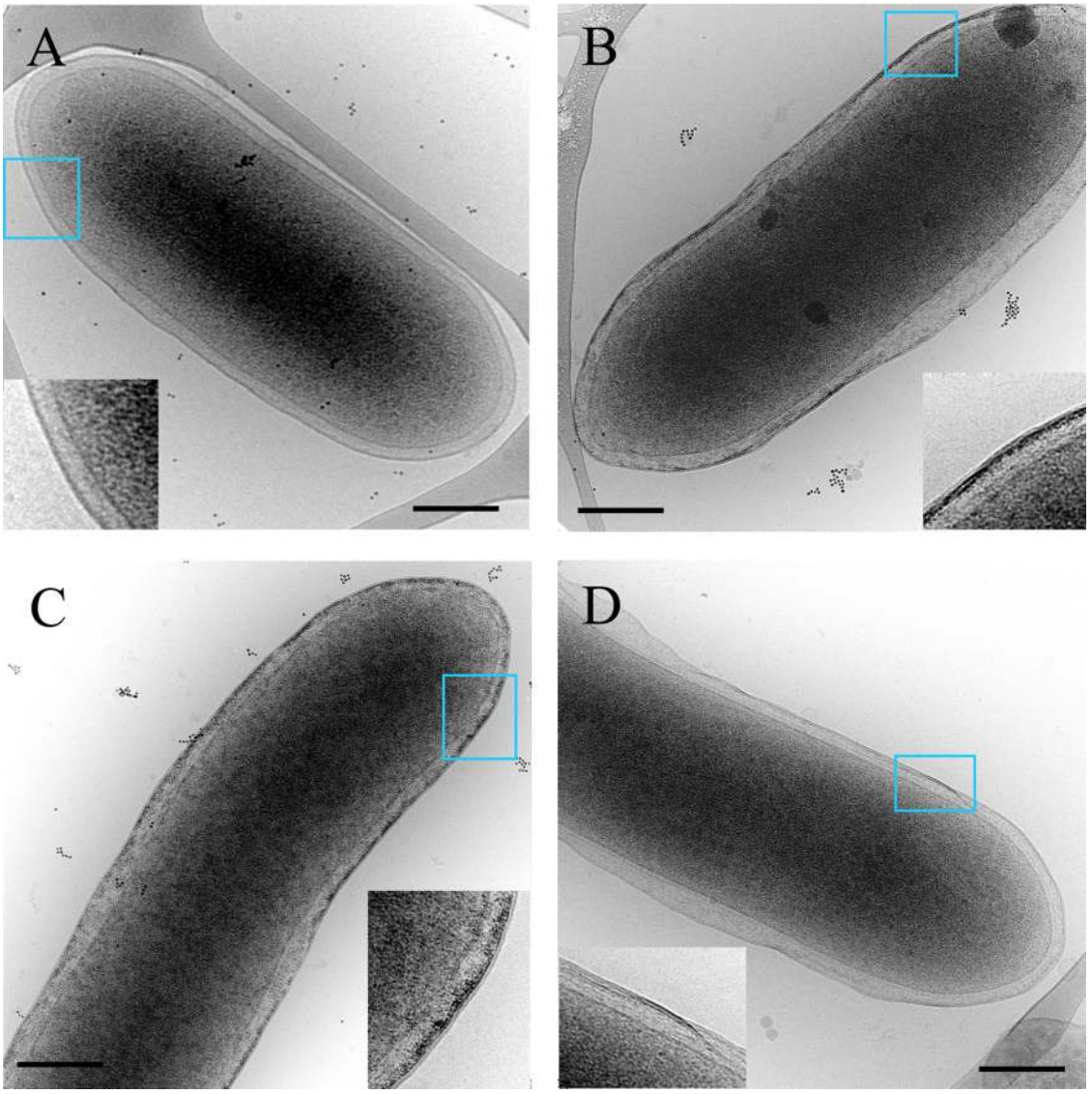

FIG 4 Cryo-TEM images of the wild type reducing fumarate (A) and of the wild type (B), Δ*pilA* mutant (C), and ΔBESTZ mutant (D) reducing U(VI). (A) The cell wall of *Geobacter* respiring in fumarate is typical of Gram-negative bacteria, with clear inner and outer membrane and a transparent periplasmic space. (B and C) The cell walls of the wild type and the Δ*pilA* mutant are spanned by irregular patches of high-contrast (electron-dense) material, mainly at the outer membrane. (D) The cell wall of the ΔBESTZ mutant respiring U(VI) appears to contain significantly less high-contrast aggregated material and is closer to that of the wild type respiring fumarate. On occasion, there are irregular patches of aggregates, as seen in the inset. Scale bar, 250 nm.

Previous studies of the mechanisms for the reduction of anthraquinone-2,6-disulfonate (AQDS), another soluble extracellular electron acceptor, demonstrated that deletion of the genes for multiple outer-surface *c*-type cytochromes was necessary in order to substantially diminish rates of AQDS reduction (6). In a similar manner, deletion of the gene for the outer-surface *c*-type cytochrome OmcB or OmcE only partially reduced rates of U(VI) reduction (26). A quadruple mutant deficient not only in OmcB and OmcE but also in the outer-surface cytochromes OmcS and OmcT still reduced U(VI) at rates of 40% of that of the wild type (Fig. 1). A quintuple mutant in which *omcZ* was deleted along with *omcB*, *omcE*, *omcS*, and *omcT* (ΔBESTZ) reduced U(VI) only at a rate 19% that of the wild type (Fig. 1). This could not be attributed solely to the loss of OmcZ, because a strain in which only *omcZ* was deleted reduced U(VI) at a rate ca. 50% of that of the wild type (Fig. 1).

Lower rates of U(VI) reduction in the quintuple mutant could not be attributed to an impact on pilus production. Transcript abundance of *pilA* relative to the housekeeping gene *proC* was 3.5-fold (±0.76-fold) higher in the quintuple mutant than in wild-type cells, and transmission electron microscopy revealed the expression of pili in the quintuple mutant and the wild type but not in the *pilA*-deficient mutant (Fig. 2; see also Fig. S1 in the supplemental material).

Species identification and localization of uranium. Analysis of cell pellets from the cell suspension incubations with X-ray absorption near-edge structure spectroscopy (XANES) demonstrated that after 4 h, 83% ± 10% of the uranium associated with

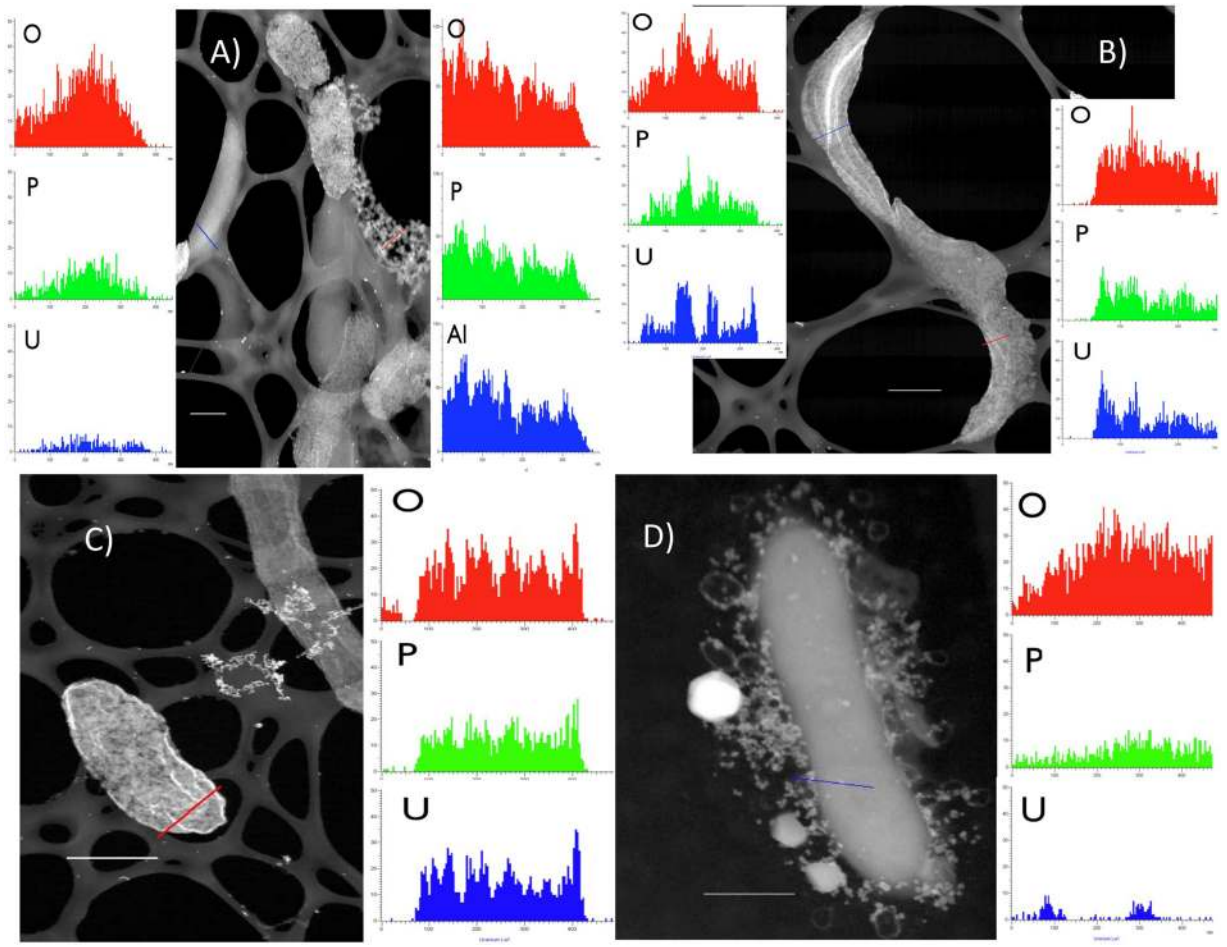

FIG 5 XEDS of the wild type (A and B), the Δ*pilA* mutant (B), or the ΔBESTZ mutant (C) respiring U(VI). High-angle annular dark-field STEM images of areas of freeze-dried cryo-TEM grids are shown. The "spider web-like" pattern supporting the cells is the lacey carbon support. The scattering from metal aggregates and gold beads appears intensely bright. The red and blue lines indicate the line scanned by the probe. Scale bar, 500 nm. Side panels show X-ray counts of the main elements along the scanned line. The units in the line scans are nm on the *x* axis and X-ray counts on the *y* axis. For O (oxygen), P (phosphorus), and Al (aluminum), it is the number of X-ray counts in their K alpha peaks, and for U, it is the number of counts in the L alpha peak. Uranium counts are significantly above the background level.

wild-type cells was U(IV), with the remainder in the U(VI) oxidation state (Fig. 3). The percentage of U(IV) was slightly lower for the *pilA* mutant (63% ± 10%), but the difference was not significant. In contrast, 89% ± 10% of uranium was present as U(VI) in the quintuple mutant (Fig. 3).

In contrast to previous reports (3), no U(IV) precipitates associated with the pili of wild-type cells were observed (Fig. 4). There was an electron-dense accumulation at the outer membrane of both the wild type and the *pilA* mutant, which X-ray energy dispersion spectroscopy (XEDS) confirmed was uranium (Fig. 5; see also Fig. S2 in the supplemental material). These precipitates were not detected in cell suspensions provided fumarate rather than U(VI) as an electron acceptor (Fig. 4A). There was very little accumulation of uranium on the outer surface of the quintuple mutant, consistent with the low levels of U(VI) reduction.

Implications. The results suggest that *G. sulfurreducens* reduces U(VI) much as it reduces AQDS, another soluble, extracellular electron acceptor. A number of outer-surface *c*-type cytochromes appear to contribute to U(VI) reduction. This is analogous to results for *Shewanella oneidensis* (25). Previous results have demonstrated that *G. sulfurreducens c*-type cytochromes, including OmcS and OmcZ, reduce U(VI) *in vitro* (18, 23). Long-range electron conduction through pili is not necessary for the reduction of other soluble electron acceptors by *G. sulfurreducens* (5) and is also not expected to be necessary for the reduction of U(VI).

ACKNOWLEDGMENTS

We thank S. Dar, M. Barlett, and P. Tremblay for helpful discussion.

This research was supported by the Office of Science (Office of Biological and Environmental Research), U.S. Department of Energy, award number DE-SC0004114. R.O. was supported by a Fulbright-CONICYT 2008 Equal Opportunities Scholarship. The work of L.R.C. and R.C. was supported by the Director, Office of Science, Office of Biological and Environmental Research, of the U.S. Department of Energy under contract no. DE-AC02-05CH11231. Work at the Molecular Foundry (EDS analysis) was supported by the Office of Science, Office of Basic Energy Sciences, of the U.S. Department of Energy under contract no. DE-AC02-05CH11231. The SLAC SFA (N.J.) was funded by the U.S. Department of Energy Office of Science (DOE-SC), Office of Biological and Environmental Research (BER), work package number 10094. SSRL is a USDOE

User Facility operated by Stanford University. The SSRL Structural Molecular Biology Program is supported by DOE-SC-BER and by the NIH Institute of General Medical Sciences (including P41GM103393) and the National Center for Research Resources (P41RR001209).

The contents of this publication are solely our responsibility and do not necessarily represent the official views of NIGMS, NCRR, or NIH. Any use of trade, product, or firm names is for descriptive purposes only and does not imply endorsement by the U.S. Government.

REFERENCES

1. **Lovley DR, Ueki T, Zhang T, Malvankar NS, Shrestha PM, Flanagan KA, Aklujkar M, Butler JE, Giloteaux L, Rotaru AE, Holmes DE, Franks AE, Orellana R, Risso C, Nevin KP.** 2011. *Geobacter*: the microbe electric's physiology, ecology, and practical applications. Adv. Microb. Physiol. **59:**1–100.
2. **Williams KH, Bargar JR, Lloyd JR, Lovley DR.** 2013. Bioremediation of uranium-contaminated groundwater: a systems approach to subsurface biogeochemistry. Curr. Opin. Biotechnol. **24:**489–497.
3. **Cologgi DL, Lampa-Pastirk S, Speers AM, Kelly SD, Reguera G.** 2011. Extracellular reduction of uranium via *Geobacter* conductive pili as a protective cellular mechanism. Proc. Natl. Acad. Sci. U. S. A. **108:**15248–15252.
4. **Reguera G.** 2012. Electron transfer at the cell-uranium interface in *Geobacter* spp. Biochem. Soc. Trans. **40:**1227–1232.
5. **Reguera G, McCarthy KD, Mehta T, Nicoll JS, Tuominen MT, Lovley DR.** 2005. Extracellular electron transfer via microbial nanowires. Nature **435:**1098–1101.
6. **Voordeckers JW, Kim BC, Izallalen M, Lovley DR.** 2010. Role of *Geobacter sulfurreducens* outer surface *c*-type cytochromes in reduction of soil humic acid and anthraquinone-2,6-disulfonate. Appl. Environ. Microbiol. **76:**2371–2375.
7. **Smith JA, Lovley DR, Tremblay P-L.** 2013. Outer cell surface components essential for Fe(III) oxide reduction by *Geobacter metallireducens*. Appl. Environ. Microbiol. **79:**901–907.
8. **Summers ZM, Fogarty HE, Leang C, Franks AE, Malvankar NS, Lovley DR.** 2010. Direct exchange of electrons within aggregates of an evolved syntrophic coculture of anaerobic bacteria. Science **330:**1413–1415.
9. **Shrestha PM, Rotaru A-E, Summers ZM, Shrestha M, Liu F, Lovley DR.** 2013. Transcriptomic and genetic analysis of direct interspecies electron transfer. Appl. Environ. Microbiol. **79:**2397–2404.
10. **Reguera G, Nevin KP, Nicoll JS, Covalla SF, Woodard TL, Lovley DR.** 2006. Biofilm and nanowire production leads to increased current in *Geobacter sulfurreducens* fuel cells. Appl. Environ. Microbiol. **72:**7345–7348.
11. **Nevin KP, Kim BC, Glaven RH, Johnson JP, Woodard TL, Methe BA, DiDonato RJ, Covalla SF, Franks AE, Liu A, Lovley DR.** 2009. Anode biofilm transcriptomics reveals outer surface components essential for high density current production in *Geobacter sulfurreducens* fuel cells. PLoS One **4:**e5628. doi:10.1371/journal.pone.0005628.
12. **Malvankar NS, Vargas M, Nevin KP, Franks AE, Leang C, Kim BC, Inoue K, Mester T, Covalla SF, Johnson JP, Rotello VM, Tuominen MT, Lovley DR.** 2011. Tunable metallic-like conductivity in microbial nanowire networks. Nat. Nanotechnol. **6:**573–579.
13. **Vargas M, Malvankar NS, Tremblay P-L, Leang C, Smith JA, Patel P, Synoeyenbos-West O, Nevin KP, Lovley DR.** 2013. Aromatic amino acids required for pili conductivity and long-range extracellular electron transport in *Geobacter sulfurreducens*. mBio **4**(2):e00210–00213. doi:10.1128/mBio.00105-13.
14. **Mehta T, Coppi MV, Childers SE, Lovley DR.** 2005. Outer membrane *c*-type cytochromes required for Fe(III) and Mn(IV) oxide reduction in *Geobacter sulfurreducens*. Appl. Environ. Microbiol. **71:**8634–8641.
15. **Leang C, Qian XL, Mester T, Lovley DR.** 2010. Alignment of the *c*-type cytochrome OmcS along pili of *Geobacter sulfurreducens*. Appl. Environ. Microbiol. **76:**4080–4084.
16. **Lovley DR.** 2011. Live wires: direct extracellular electron exchange for bioenergy and the bioremediation of energy-related contamination. Energy Environ. Sci. **4:**4896–4906.
17. **Lovley DR.** 2012. Long-range electron transport to Fe(III) oxide via pili with metallic-like conductivity. Biochem. Soc. Trans. **40:**1186–1190.
18. **Inoue K, Qian XL, Morgado L, Kim BC, Mester T, Izallalen M, Salgueiro CA, Lovley DR.** 2010. Purification and characterization of OmcZ, an outer-surface, octaheme *c*-type cytochrome essential for optimal current production by *Geobacter sulfurreducens*. Appl. Environ. Microbiol. **76:**3999–4007.
19. **Inoue K, Leang C, Franks AE, Woodard TL, Nevin KP, Lovley DR.** 2011. Specific localization of the *c*-type cytochrome OmcZ at the anode surface in current-producing biofilms of *Geobacter sulfurreducens*. Environ. Microbiol. Rep. **3:**211–217.
20. **Qian XL, Reguera G, Mester T, Lovley DR.** 2007. Evidence that OmcB and OmpB of *Geobacter sulfurreducens* are outer membrane surface proteins. FEMS Microbiol. Lett. **277:**21–27.
21. **Leang C, Coppi MV, Lovley DR.** 2003. OmcB, a *c*-type polyheme cytochrome, involved in Fe(III) reduction in *Geobacter sulfurreducens*. J. Bacteriol. **185:**2096–2103.
22. **Leang C, Adams LA, Chin KJ, Nevin KP, Methe BA, Webster J, Sharma ML, Lovley DR.** 2005. Adaptation to disruption of the electron transfer pathway for Fe(III) reduction in *Geobacter sulfurreducens*. J. Bacteriol. **187:**5918–5926.
23. **Qian XL, Mester T, Morgado L, Arakawa T, Sharma ML, Inoue K, Joseph C, Salgueiro CA, Maroney MJ, Lovley DR.** 2011. Biochemical characterization of purified OmcS, a *c*-type cytochrome required for insoluble Fe(III) reduction in *Geobacter sulfurreducens*. Biochim. Biophys. Acta **1807:**404–412.
24. **Lovley DR, Widman PK, Woodward JC, Phillips EJP.** 1993. Reduction of uranium by cytochrome c3 of *Desulfovibrio vulgaris*. Appl. Environ. Microbiol. **59:**3572–3576.
25. **Marshall MJ, Beliaev AS, Dohnalkova AC, Kennedy DW, Shi L, Wang ZM, Boyanov MI, Lai B, Kemner KM, McLean JS, Reed SB, Culley DE, Bailey VL, Simonson CJ, Saffarini DA, Romine MF, Zachara JM, Fredrickson JK.** 2006. c-Type cytochrome-dependent formation of U(IV) nanoparticles by *Shewanella oneidensis*. Plos Biol. **4:**e268. doi:10.1371/journal.pbio.0040268.
26. **Shelobolina ES, Coppi MV, Korenevsky AA, DiDonato LN, Sullivan SA, Konishi H, Xu HF, Leang C, Butler JE, Kim BC, Lovley DR.** 2007. Importance of c-type cytochromes for U(VI) reduction by *Geobacter sulfurreducens*. BMC Microbiol. **7:**16. doi:10.1186/1471-2180-7-16.
27. **Comolli LR, Duarte R, Baum D, Luef B, Downing KH, Larson DM, Csencsits R, Banfield JF.** 2012. A portable cryo-plunger for on-site intact cryogenic microscopy sample preparation in natural environments. Microsc. Res. Tech. **75:**829–836.
28. **Downing KH, Mooney PE.** 2008. A charge coupled device camera with electron decelerator for intermediate voltage electron microscopy. Rev. Sci. Instrum. **79:**043702–043710.
29. **Kremer JR, Mastronarde DN, McIntosh JR.** 1996. Computer visualization of three-dimensional image data using IMOD. J. Struct. Biol. **116:**71–76.
30. **Ravel B, Newville M.** 2005. Athena, Artemis, Hephaestus: data analysis for X-ray absorption spectroscopy using Ifeffit. J. Synchrotron Radiat. **12:**537–541.
31. **Holmes DE, Nevin KP, O'Neil RA, Ward JE, Adams LA, Woodard TL, Vrionis HA, Lovley DR.** 2005. Potential for quantifying expression of the *Geobacteraceae* citrate synthase gene to assess the activity of *Geobacteraceae* in the subsurface and on current-harvesting electrodes. Appl. Environ. Microbiol. **71:**6870–6877.